CHAPTER 6

A MATHEMATICAL MODEL FOR THE LONG RANGE HYDROPHOBIC FORCE

6.1 INTRODUCTION

The DLVO theory states that the interaction force between lyophobic particles in aqueous media is given by the algebraic sum of the electrical double layer force (F_e) and the van der Waals force (F_d) [1,2]:

$$F = F_e + F_d \qquad [1]$$

However, Israelachvili and Pashley [3,4] observed that the forces of interaction between cylindrical mica sheets in 1×10^{-5} M cetyltrimethyl ammonium bromide (CTAB) solutions is more attractive than those predicted by the DLVO theory. These investigators represented the extra attractive force using:

$$\frac{F_h}{R} = C_o \exp(\frac{-H}{D_o}) \qquad [2]$$

where R is the mean radius of curvature of the interacting surfaces, H the closest separation distance, C_o and D_o are fitting parameters. The parameter D_o has a unit of length and, hence, is known as the decay length. The hydrophobic force observed by Israelachvili and Pashley was fitted to Eq. [2] with C_o =-140 mN/m and D_o=1.0 nm.

When stronger hydrophobic forces were measured, a double exponential function [5-6]:

$$\frac{F_h}{R} = C_1 \exp(\frac{-H}{D_1}) + C_2 \exp(\frac{-H}{D_2}) \qquad [2]$$

was found to better fit the experimental data. In effect, C_1 and D_1 represent the short range attraction, while C_2 and D_2 represent the long range attraction. Note that Eq.[2] uses four parameters (C_1, C_2, D_1 and D_2) that can be varied to fit the data.

Some investigators prefer to fit the measured hydrophobic forces using power law [7,8]:

$$F_h = \frac{-KR}{6H^2} \qquad [3]$$

in which K is the only fitting parameter. Eq.[3] is the of the same form as the van der Waals force. Therefore one can directly compare K with the Hamaker constant A.

Over the years, hydrophobic forces have been measured between various macroscopic surfaces that have been hydrophobized using different procedures. These include equilibrium adsorption of ionic surfactants from aqueous solution [3,4], equilibrium adsorption of surfactants from non-aqueous solvents [9-11], Langmuir-Blodgett (LB) deposition of insoluble double chain surfactants [5,6] and chemical modification of surfaces [7,8]. In general, LB deposited films or chemically modified surfaces exhibit stronger hydrophobic forces than the equilibrium adsorbed surfactants [12]. However, there are exceptions to this generalization [13-15].

Hydrophobic forces are now routinely measured between various macroscopic hydrophobic surfaces. However its molecular origin remains unclear. A number of mechanisms have been suggested so far. These theories of hydrophobic forces may be grouped into those based on electrostatic mechanisms and those based on non-electrostatic mechanisms. According to the former, the long range attraction between hydrophobic surfaces may be due to: i) an anomalous polarization fluctuation in the film adjacent to a hydrophobic surface [16], ii) a fluctuating electric field due to lateral mobility of adsorbed counter ions [17], iii) correlation of dipoles due to domain formation of the adsorbed surfactant films [7, 18], and iv) an attractive double-layer force due to non uniform charge distribution in net neutral surfaces [19]. An

important test for the theories based on electrostatic mechanisms is that the range of the interaction should decrease with increasing electrolyte concentration [13]. Unfortunately, the effect of electrolyte on the magnitude of the hydrophobic force remains quite controversial. The magnitudes of the experimentally measured hydrophobic force have been shown to increase [20], decrease [9] or remain unaffected [13] with increase in electrolyte concentration. Hence, theories based on electrostatic mechanisms do not receive unequivocal support.

According to the theories based on non-electrostatic mechanisms, the long range attraction may be due to: i) formation of a vapor cavity [21, 22], ii) submicroscopic density or thermal fluctuations [23, 24], iii) hydrodynamic fluctuations [25,26], iv) nucleation of air bubbles dissolved in water [14, 27], v) a bridging effect due to a captured air bubble [28], vi) adsorption/desorption equilibrium of surfactants [29, 30] and vii) structural effects due to ordering of water molecules [31]. The non electrostatic mechanisms suggest only a weak dependence on electrolyte concentration.

According to the theories suggested above the magnitude of the hydrophobic force should increase with increasing hydrophobicity of the surface. Yoon and Ravishankar [32,33] found that the magnitude of the hydrophobic force increased significantly for surfaces exhibiting contact angle greater than 90^o. They suggested that for lower contact angles ($\theta_a<90^o$) mechanisms such as dipole correlation due to domain formation may result in an attractive force. For surfaces exhibiting higher contact angles ($\theta_a>90^o$) both dipole correlation and cavitation may occur simultaneously to result in long range attraction. However, the role of hydrophobicity on the magnitude of the hydrophobic force has remained controversial since certain extremely hydrophobic surfaces such as teflon or polystyrene do not exhibit a long range attraction [9, 34].

In the present work, a theory has been proposed for the long-range hydrophobic forces. It is based on a mechanism suggested by Rabinovich et al [18] that the long range attraction may be due to correlation of the dipoles of hydrophobic domains. These investigators subscribed to the theory that water molecules on hydrophobic surfaces are unidirectionally oriented, which in

turn gives rise to large dipole moments. If a hydrophobic surface consists of domains of adsorbed hydrocarbon chains, the dipole moment should vary depending on the domains size and the orientation of the hydrocarbon chains. A mathematical model has been developed based on this theory. The model parameter was determined by fitting it to experimental force curves obtained under different conditions.

6.2 THEORY

Figure 6.1 shows a schematic representation of two infinitely flat surfaces aligned parallel to each other. The surfaces are assumed to be immersed in a polar solvent such as water. It is the purpose of the present work to seek an expression for the total electrostatic interaction energy per unit area between the two surfaces as a function of the distance, *H*, separating them. The squares in each surface are assumed to represent hydrophobic domains on which the water molecules are unidirectionally oriented resulting in giant dipole moments (Figure 6.1 (a)). Therefore, each square in Figure 6.1 may be assumed to represent one giant dipole with a very large dipole moment.

We shall begin our treatment by making the following assumptions:

(1) All the domains on each surface are square shaped with a characteristic length of each side is 2 R_d, i.e., area of each domain is $4R_d^2$.

(2) The interaction energy ($w(r)$)between a domain on Surface I with a domain on Surface II is in the form of a simple function like:

$$w(r) = \frac{-C}{r^n} \qquad [3]$$

where C is a constant and r is the separation distance between the two domains.

(3) The interaction energies of all the domains between the two surfaces are pair wise additive.

Let us begin by considering the interaction energy of one domain *B* on Surface II with all the domains on Surface I. Using Eq. [3] the interaction energy $w_{A\text{-}B}$ between Domain *B* on Surface II and a domain *A* on Surface I that is perpendicularly opposite to it and separated by a distance *H* apart is given by:

$$w_{A-B} = \frac{-C}{H^n} \qquad [4]$$

Equation [4] can be used to calculate the interaction energy (w_1) between domain *B* and all the domains in Row 1 of Surface I (see Figure 6.1). This is readily calculated since the separation distance between domain *B* and any other domain in Row 1 can be determined in terms of the perpendicular distance of separation *H* and the length of each square (=$2R_d$)

Therefore the total interaction energy (w_1) for all the domains in Row 1 of Surface I interacting with domain *B* on surface II is given by:

$$w_1 = -C\left[\frac{1}{H^n} + \frac{2}{\left((2R_d)^2 + H^2\right)^{n/2}} + \frac{2}{\left((4R_d)^2 + H^2\right)^{n/2}} + \frac{2}{\left((6R_d)^2 + H^2\right)^{n/2}} + ...\right] \qquad [5]$$

Note that in the above expression a factor "2" appears in all the terms except the first one since for every domain to the left of the domain *A*, there exists a domain that is symmetrically placed to the right of domain *A* which interacts equally with domain *B*.

Similarly, one can use the same approach to calculate the interaction energy terms for all the domains in row 2 (w_2) and row 3 (w_3) on surface I with domain *B*. For the interaction of domain *B* with all the domains in Row 2, we obtain:

$$w_2 = -C\left[\frac{1}{\left((2R_d)^2 + H^2\right)^{n/2}} + \frac{2}{\left((2R_d)^2 + (2R_d)^2 + H^2\right)^{n/2}} + \frac{2}{\left((4R_d)^2 + (2R_d)^2 + H^2\right)^{n/2}} + ...\right] \qquad [6]$$

Similarly for the interaction of domain *B* with all the domains in Row 3, we have:

$$w_3 = -C\left[\frac{1}{\left((4R_d)^2 + H^2\right)^{n/2}} + \frac{2}{\left((4R_d)^2 + (2R_d)^2 + H^2\right)^{n/2}} + \frac{2}{\left((4R_d)^2 + (4R_d)^2 + H^2\right)^{n/2}} + ...\right] \quad [7]$$

Therefore, the total interaction energy (*w*) between domain *B* and all the rows of domains on surface I. is given by:

$$w = w_1 + 2w_2 + 2w_3 + ...2w_x + ... \quad [8]$$

where w_x represents the interaction of domains in any row "*x*" interacting with domain *B.* Note that the factor 2 appears again since for every row 2 above row 1, there exists a row 2' that lies symmetrically below row 1.

Using Eq. [8] a generalized equation for the net interaction energy (*w*) for all the domains in surface I interacting with domain *B* can be conveniently summed as:

$$w = -C\left[\frac{1}{H^n} + \sum_{k=1}^{\infty} \frac{4}{\left((2kR_d)^2 + H^2\right)^{n/2}} + \sum_{s=1}^{\infty}\sum_{t=1}^{\infty} \frac{4}{\left((2sR_d)^2 + (2tR_d)^2 + H^2\right)^{n/2}}\right] \quad [9]$$

Recall that domain *B* is only one of the many domains on Surface II. Also the interaction energy of any one domain on surface II with those on Surface I will be given by the same expression as Eq. [9]. Thus the total interaction energy between all the domains on each surface will be n*w*, n being the number of domains on each surface. Dividing it by the area of each surface nA_D, where A_D is the area of each domain, one obtains the interaction energy per unit area (*W(H)*):

$$W(H) = \frac{w}{A_D} \quad [10]$$

An advantage of obtaining an expression in terms of the interaction energy per unit area between two flat plates is that the Derjaguin approximation can be applied to convert it into an expression of force per unit length. For the specific case of a sphere of radius *R* interacting with a flat plate one obtains [33]:

$$\frac{F}{R} = 2pW(H) \qquad [11]$$

Eq. [11] will enable one to directly compare the theoretical predictions of the model with the measured force data.

Finally, it needs to be pointed out that the constant "C" in Eq. 9 still remains undefined. Since the constant essentially depends on the functional form of *w(r)* (Eq. [3]) the question arises as to what is the most appropriate form of *w(r)* that needs to be used. We shall treat it in the simplest way as an interaction between two dipoles that are aligned in an anti parallel fashion so that it becomes net attraction. The functional form of w(r) used in the present work is given by [35]:

$$w(r) = \frac{-m_1 m_2}{4pe_o eH^3} \qquad [12]$$

where μ_1 and μ_2 are the individual dipole moments, ε_o is the permittivity of free space ($=8.85\times10^{-12}$) and ε is the dielectric constant of the medium [35]. From Eqs.[3] and [12], $C = \mu_1\mu_2/4\pi\varepsilon_0\varepsilon$ and n=3.

From Eqs. [9] to [12] in Eq. [11] and assuming that $\mu_1=\mu_2=\mu$, one obtains the following:

$$\frac{F_h}{R} = -\frac{m^2}{2A_D e_o e}\left[\frac{1}{H^3} + \sum_{k=1}^{\infty} \frac{4}{\left((2kR_d)^2 + H^2\right)^{3/2}} + \right.$$

$$+\sum_{s=1}^{\infty}\sum_{t=1}^{\infty}\frac{4}{\left((2sR_d)^2+(2tR_d)^2+H^2\right)^{3/2}}\Bigg] \qquad [13]$$

Note that if the domain size ($2R_d$) is known the one can fit the attractive force obtained from Eq. [13] to experimental force curves by choosing appropriate values of the dipole moment (μ).

6.3 EXPERIMENTAL

6.3 (a) Materials

Optically smooth fused silica plates were obtained from Haraeus Amersil, Inc., and cleaned by boiling in nitric acid solution for 12-15 h before use. Glass spheres obtained from Duke Scientific were used as received. HPLC grade cyclohexane was obtained from Aldrich Chemical Company at 98% purity and used as received. Octadecyltrichlorosilane (OTS) was also obtained from Aldrich Chemical Company at 95% purity and used without further purification. All experiments were conducted using conductivity water produced from a Barnstead Nanopure II water treatment unit.

6.3 b Apparatus and Procedure

Surface force measurements between a silanated glass sphere and an OTS-coated flat silica plate were conducted using a Digital Instruments Nanoscope III atomic force microscope (AFM). The glass sphere was glued to the end of an AFM cantilever spring by means of Epon R Resin 1004F obtained from Shell Chemicals Company in a manner described by Ducker et al [34]. The AFM was equipped with a standard liquid cell. All AFM force measurements were carried out in a manner described by Rabinovich and Yoon [7]. For the measurement of weak

repulsive forces standard triangular silicon nitride (Si_3N_4) cantilevers ($0.1<k<0.32$ N/m) were used while rectangular TESP cantilevers ($25<k<35$ N/m) were used to measure strong attractive forces. The cantilevers were calibrated using the technique described by Cleveland et al [37].

6.3 c Silanation

Fused silica plates were silanated in OTS-in-cyclohexane solutions in a nitrogen atmosphere. The cyclohexane was dried overnight over 3-12 mesh Davidson 3-Å molecular sieves before use. Flinn et al [38] described the process of silanation in detail. The hydrophobicity of the silica plates could be varied by choosing appropriate concentrations of OTS and by changing the immersion times [38]. For force measurements, glass spheres were silanated along with the silica plates in the same batch, so that the plates and the spheres exhibited identical hydrophobicities.

6.4 RESULTS AND DISCUSSION

Figure 6.2 shows the results of a series of force measurements obtained for the interaction between symmetric silanated surfaces, i.e., the silica plates and the glass spheres were silanated under identical conditions. This would give the two surfaces the same degree of hydrophobicity and, hence, the same contact angle (θ_a). The measured forces (F), normalized by the radius of the sphere (R), are plotted versus the separation distance (H).

There are four different force curves shown in Figure 6.2. They were obtained between surfaces with θ_a = 0, 75, 83 and 92°. The dotted line in Figure 6.2 represents a theoretical DLVO fit of the data obtained at θ_a=0°. The ion electrostatic force (F_e) was calculated using the constant potential model of Oshima et al [37] with ψ_1(surface potential) = −60 mV and κ^{-1} (Debye length) = 94. The Lifshitz Van der Waals force (F_d) was calculated using $A_{131}=8\times10^{-21}$ J,

which was taken from literature [40]. Since ψ_1 does not change with silanation of silica [41], the dotted line (Figure 6.1) may represent the DLVO fit for all the force curves given in Figure 6.2.

Note that all the force curves shown in Figure 6.2 cannot be fitted to the DLVO theory. The results obtained at θ_a =0^o show an extraneous repulsive force which has been attributed to the hydration of the silica surfaces [42]. On the other hand, the force curves obtained at θ_a =75, 83 and 92^o show an extra attractive force not accounted for by the DLVO theory. Derjaguin and Chuarev [43] have suggested that the DLVO theory is only applicable to weakly hydrophobic colloids that exhibit contact angles in the range of 20-45^o.

The solid lines in Figure 6.2 represent an extended DLVO fit of the data to the extended DLVO theory:

$$F = F_e + F_d + F_h \qquad [14]$$

where F_h represents the contributions from the hydrophobic force. The values of F_e and F_d used are the same as those used for θ_a=0^o. In the present work, the values of F_h were calculated using Eq. [13] by choosing appropriate values of the dipole moments and domain size. Equation [13] was solved using a mathematical software called *Mathcad* [44].

As Figure 6.2 shows the measured force data can be fitted very well using the extended DLVO theory. In other words Eq. [13] can fit the hydrophobic forces measured at $\theta_a \leq 92^o$. Of the two fitting parameters the dimension of each domain has been assumed to be equal to 20nm×20 nm, as has been shown to be the case with OTS adsorbed on silica. The dipole moment used to fit the experimental data are: 1×10^3, 1.5×10^3 and 8×10^3 D (1D=3.36×10^{-30} Cm) for surfaces exhibiting θ_a of 75, 83, and 92^o respectively (see Table 6.1).

Note that the hydrophobic forces shown in Figure 6.2 have been fitted by assuming that the area of the domain does not increase with silanation; only the values of the dipole moment

increases. Flinn et al [38] studied the adsorption of OTS on silica using atomic force microscopy and FTIR spectroscopy. These authors found that OTS begins to adsorb in patches or domains on the surface of silica. With increasing silanation, the size of the patch remains the same; however the adsorption density of OTS molecules within each patch increases. The increase in the adsorption density of OTS resulted in a well ordered hydrocarbon layer that exposed its terminal methyl groups to the aqueous phase. The CH_3 groups may present an ordered layer of dipoles to which the adjacent water dipoles may respond. Therefore as the ordering of the hydrocarbon chains within a domain increases it is expected that the adjacent water dipoles get increasingly aligned, thereby resulting in increased values of dipole moments.

Figure 6.3 shows the force measurements conducted between silanated silica surfaces with θ_a of 100, 105 and 109°. Note that the hydrophobic force measured for these conditions is much stronger than those observed in Figure 6.2. The solid lines represent an extended DLVO fit in which Eq. [13] is used to represent F_h. The force data have been fitted to the extended DLVO theory using $\mu=1\times10^4$, 2.5×10^4 and 3.5×10^4 D for θ_a = 100, 105 and 109° respectively. Note that the value of μ used to fit the data obtained at θ_a=109° is an order of magnitude higher than the value used to fit the data obtained at θ_a=75° ($\mu=1\times10^3$ D).

It can be readily seen from Figure 6.3 that while the predictions of the theoretical model agree well with the measured force data at large separation distances, significant deviations occur at shorter separations. A possible explanation may be that an additional attractive force may be present at shorter separations due to mechanisms that have not been considered in the development of the present model. Take, for example, mechanisms such as cavitation, which may be operating in tandem with the one suggested here. In fact, it is well known that the formation of a vapor cavity becomes thermodynamically favorable for surfaces of $\theta_a > 90°$ [22]. Molecular simulation studies suggested that interaction between two surfaces in a poorly wetting liquid will result in long range attraction due to cavitation [45]. Furthermore, the formation of a vapor cavity has been observed either directly or inferred between hydrophobic surfaces [22, 20].

There are three important features in Figure 6.3 that support the idea that the deviations seen in Figure 6.3 are due to cavitation. *One*, all the surfaces in Figure 6.3 exhibit θ_a much greater than 90^o. Hence, cavitation should occur thermodynamically. *Two*, the deviation between the theoretical prediction and the experimental data increases with increasing contact angle. It has been shown that with increasing hydrophobicity not only does the likelihood of the formation of a vapor cavity increases, but also the size of the cavity formed [22]. *Three*, the deviations observed in Figure 6.3 increase with decreasing separation distance (H) between the surfaces. This again is indicative of a cavitation mechanism at play since the activation energy required for the formation of a cavity decreases with decrease in separation distance [21].

Figure 6.4 shows the dipole moments obtained in Figures 2 and 3 plotted as a function of the advancing contact angle θ_a. Note that the values of dipole moment used to fit the hydrophobic force data increase by an order of magnitude for surfaces of $\theta_a > 90^o$. The increase in dipole moment can be directly related to the increase in the magnitude of the hydrophobic force (Also shown in Figure 6.4). In this context, it is necessary to discuss the work of Yoon and Ravishankar [32,33]. These authors conducted force measurements between cylindrical mica sheets in dodecyl ammonium hydrogen chloride (DAHCl) solutions in the presence of neutral surfactants such as octanol or dodecanol. They found that the magnitude of the hydrophobic force increased drastically at $\theta_a \geq 90^o$. Yoon and Ravishankar [33] argued that two entirely different mechanisms may simultaneously be at play resulting in long range attraction. The first mechanism they suggested is the one considered here, i.e., dipolar correlation due to giant dipoles of unidirectionally oriented water molecules. According to Yoon and Ravishankar [33], as surfaces become hydrophobic ($\theta_a > 90^o$) they form a well-ordered monolayer of hydrocarbon chains which tend to expose their methyl groups to the aqueous solution. As mentioned earlier, the CH_3 groups may present an ordered layer of dipoles to which the adjacent water dipoles may respond. This may result in an increased orientation of the water molecules resulting in giant dipoles. In Figure 6.4, the increase in dipole moment at $\theta_a > 90^o$ essentially support these claims.

The second mechanism suggested by Yoon and Ravishankar [33] was based on the observation that the magnitude of the hydrophobic force showed a transition at θ_a=90°. This was strongly indicative of a cavitation-like mechanism. Recall that the hydrophobic force calculated based on dipolar correlation alone is unable to describe the long range hydrophobic force satisfactorily (Figure 6.3). In other words, as suggested by Yoon and Ravishankar [33], both the mechanism of dipolar correlation and cavitation should be considered when discussing the molecular origin of the long range hydrophobic force.

If we were to assume that a cavitation-like mechanism also contributes to the long range attraction observed in the present work, then the net hydrophobic forces (F_h) shown in Figure 6.3 may be represented as an algebraic sum:

$$F_h = C_o \exp(\frac{-H}{D_o}) - \frac{m^2}{2A_D \varepsilon_o \varepsilon}\left[\frac{1}{H^3} + \sum_{k=1}^{\infty} \frac{4}{\left((2kR_d)^2 + H^2\right)^{3/2}} + \right.$$

$$\left. + \sum_{s=1}^{\infty}\sum_{t=1}^{\infty} \frac{4}{\left((2sR_d)^2 + (2tR_d)^2 + H^2\right)^{3/2}}\right] \quad [15]$$

where the first expression (exponential) may represent contributions from mechanisms such as cavitation and the second expression represents contributions from dipole correlation (Eq.[13]) due to domain formation.

Figure 6.5 shows the experimental data points obtained for silanated silica surfaces with θ_a=100, 105 and 109°. The solid lines show the extended DLVO theory fit in which F_h has been calculated using Eq. [15]. The C_o and D_o values used for obtaining the fit are given in Table 6.1. (The contributions to the hydrophobic force from dipole correlation have been assumed to be the same as in Figure 6.3). The C_o and D_o values obtained agree well with values reported in literature for hydrophobic forces where cavitation has been directly observed [12]. It can be readily seen from Figure 6.5 that incorporating a term for cavitation provides an excellent fit to

the hydrophobic force data. In essence, Figure 6.5 suggests that both dipole correlation and cavitation need to be considered while discussing the molecular origin of the long-range attractive force.

Finally, there are certain aspects of the model that need to be addressed in detail. *Firstly,* are the large values of dipole moments used for data fitting realistic? It needs to be emphasized that the theory proposed here is based on the premise that the water molecules adjacent to hydrophobic domains align unidirectionally to result in giant dipoles. Molecular simulation studies of water molecules adjacent to a hydrophobic surface indeed do show that they are aligned in a parallel fashion [44,45]. Evidence for a unidirectional orientation also comes from the electrooptical studies of Tolstoi and coworkers [46,47]. More importantly Tolstoi and coworkers [48,49] found that such orientation of water molecules on lyophobic colloidal particles can result in dipole moments as large as 1×10^{10} D (In comparison the dipole moment of one water molecule is equal to 1.85 D). Hence, the values of dipole moments used in the present work are very reasonable.

Secondly, what is the effect of such large dipoles on the intervening medium? Do the water molecules in between get polarized? Let us consider the case of a water molecule close to a silanated surface exhibiting θ_a=109^o at a distance of 5 nm away from the surface. One can calculate the interaction energy between the hydrophobic surface and the water molecule using Eq. [9]. By assuming a dipole moment value of 1.85 D for water and a dipole moment value of 3.5×10^4 for each domain, the net interaction energy is calculated to be equal to 7.45×10^{-22} J, which is equal to 0.18 kT (at 298 K). In other words, this interaction energy is much less than kT suggesting that the water molecules at distances of 5 nm will not be polarized effectively due to the large dipole moments [35].

Conversely, we can equate the interaction energy from Eq. [9] to kT and solve for the distance H at which a water molecule will get polarized. Such a calculation reveals that for H=2.65 nm the interaction energy becomes equal to kT, i.e., only the water molecules within the

first 2.5 nm adjacent to the surface will get polarized. Assuming that a water molecule has a diameter of 0.28 nm [35], a distance of 2.65 nm would approximately contain 9 layers of water molecules. In other words, all the water molecules after the first 9 layers should attain their bulk characteristics. This is in excellent agreement with molecular simulation studies that suggest that water attains its bulk characteristics within 10 molecular diameters from a hydrophobic surface [46, 47].

6.5 CONCLUSIONS

A mathematical model was developed for the correlation of the large dipoles formed on opposing surfaces coated with surfactant molecules in aqueous media. The model is based on the premise that the attraction between the correlating dipoles may be the origin of the hydrophobic forces measured in experiment. An expression for the hydrophobic force has been derived explicitly in terms of the dipole moment, the domain size and the separation distance between the two interacting surfaces.

The model was used to fit the hydrophobic forces measured as a function of the separation distance between silanated silica surfaces by using the dipole moment as an adjustable parameter and using the values of the domain sizes reported in the literature. The results show that the hydrophobic forces measured at contact angles below approximately 90^o can be adequately described by the model. For surfaces exhibiting higher contact angles, the measured hydrophobic forces can be fitted to the model only at large separation distances. As shorter separation distances, it is necessary to include another mechanism, i.e., cavitation, to adequately fit the measured hydrophobic forces.

.

6.6 REFERENCES

1. Derjaguin, B.V., and Landau, L., *USSR Acta Physiochim*. **14**, 633 (1941)
2. Verwey, E.J., and Overbeek, J.Th.G., "Theory of the Stability of Lyophobic Colloids, Elsevier, New York, 1947
3. Israelachvili, J., and Pashley, R.M., *Nature*, **300**, 341 (1982)
4. Israelachvili, J., and Pashley, R.M., *Colloids and Surfaces*, **2**, 169 (1981)
5. Claesson, P.M., Blom, C., Herder, C.E., and Ninham, B.W., *J.Colloid Interface Sci.* **114**, 234 (1986)
6. Claesson, P.M., and Christenson., H.K., *J.Phys. Chem*., **92**, 1650 (1988
7. Rabinovich, Ya. I., and Yoon, R-H, *Langmuir*, **93**,263 (1994).,
8. Yoon, R-H., Flinn, D.H., and Rabinovich, Ya.I., *J.Colloid Interface Sci.*, **185**, 179 (1997)
9. Tsao, Y-H., Evans, D.F., and Wennerstrom, H., *Science*, **262**, 547 (1993)
10. Tsao, Y-H, Evans, F.D., and Wennerstrom, H., *Langmuir*, **9**, 779 (1993).
11. Tsao, Y-H, Evans, F.D., and Wennerstrom, H., *Langmuir*, **7**, 3154 (1991).
12. Christenson,H.K., In: *Modern Approaches to Wettability.*, Eds: Schrader, M.E., and Loeb., G.I., Plenum Press, 1992
13. Craig, V.S.J., Ninham, B.W., and Pashley, R.M., *Langmuir*, **14**, 3326 (1998).
14. Craig, V.S.J., Ninham, B.W., and Pashley, R.M., *Langmuir*, **15**, 1562 (1999).
15. Parker, J.L., and Claesson, P.M., Languir, 10, 635 (1994).
16. Attard, P., *J.Phys.Chem*., **93**, 6441 (1989).
17. Podgornik, R., *J.Chem. Phys.*, **91**, 5840 (1989).
18. Rabinovich, Ya., Guzonas, D., and Yoon, R-H., *Langmuir*, **9**, 1168, (1991).
19. Miklavic, S.J., Chan, D.Y.C., White, L.R., and Healy, T.W., J. Phys. Chem., 98, 9022 (1994)
20. Parker, J.L., Claesson, P.M., Attard, P., *J.Phys. Chem*., **98**, 8468 (1994).
21. Yaminsky, V.V., Yushchenko, V.S., Amelina, E.A., and Shchukin, D., *J. Colloid and Interface Sci*., **96**, 301 (1983).
22. Christenson and Claesson, *Science*, **239**, 390 (1988).
23. Yaminsky, V.V., and Ninham, B., *Langmuir*, **9**, 3618 (1993).
24. Forsman, J., Jonsson, B., Woodward, C.E., and Wennerstrom, H., *J.Phys.Chem*., **101**, 4253 (1997).
25. Ruckenstein, E., and Churaev, N., *J.Colloid and Interface Sci*., **147**, 535 (1991).
26. Ruckenstein, E., *J.Colloid and Interface Sci*., **188**, 218 (1997).
27. Carambassis, A., Jonker, L.C., Attard, P., and Rutland, M., *Physical Review Letters*, **80**, 5357 (1998).
28. Attard, P., Langmuir, 12, 1693 (1996).
29. Yaminsky, V.V., Ninham, B.W., Christenson, H.K., Pashley, R.M., *Langmuir*., **12**, 1936 (1996).
30. Christenson, H.K., and Yaminsky, V.V., *Colloids and Surfaces*.,**129**, 67 (1997).
31. Eriksson, J.C., Ljungrenn, S., Claesson, P.M., *J.Chem.Soc., Faraday Trans.2*., **85**, 163 (1989).
32. Yoon, R-H., and Ravishankar, S.A., *J.Colloid Interface Sci.* **166**, 215 (1994)
33. Yoon, R.-H., and Ravishankar, S. A., *J.Colloid Interface Sci.* **179**, 391 (1996).

34. Meagher, L., and Craig, V.S., *Langmuir*, **10**, 2736 (1994).
35. Israelachvili, J., *Intermolecular and Surface Forces*, 2nd Edition, Academic Press, (1992).
36. Ducker, W.A., Senden, T.J., and Pashley, R.M., *Nature*, **353**, 239, (1991).
37. Cleveland , J.P., Manne, S., Bocek, D., Hansma, P.K., Rev. Sci. Instrum. 64, 1 (1993).
38. Flinn, D. H., Guzonas,D. A., and Yoon, R.-H., *Colloids and Surfaces*, **87**, 163 (1994).
39. Oshima, H., Healy, T.W., and White, L.R., *J.Colloid Interface Sci.* **185** 363 (1997
40. Hough, D.B., and White, L.R., *Adv. Colloid Interface Sci.*, **14** 3 (1980).
41. Laskowski, J., and Kitchener, B.K., *J.Colloid Interface Sci.* **166**, 215 (1994)
42. Peschel, G., Belouschek, P., Muller, M.M., Muller, M.R., Konig, R., *Colloid Polym. Sci*., 260, **444** (1982)
43. Derjaguin, B.V., and Churaev, N.V., *J.Colloid Interface Sci.*, **103,**542 (1985)
44. Mathcad
45. Berard, D.R., Attard, P., and Patey, G.N., J.*Chem. Phys*., **98**, 7236 (1993)
46. Lee, C.Y., McCammon, J.A., and Rossky, P.J., *J.Chem. Phys.*, **80 (9),** 4448, (1984).
47. Christou, N.I., Whitehouse, J.S., Nicholson, D., and Parsonage, N.G., *Mol. Phys*.,**55**, 397 (1985).
48. Tolstoi, N.A., Spartakov, A.A., Trusov, A.A., and Khilko, G.I., *Kolloidnyi Zhurnal*, **28**, 881 (1966).
49. Tolstoi, N.A., Spartakov, A.A., Trusov, A.A., and Schelkunova, S.A., *Biophysics*, **11**, 515 (1966)

Table 6.1. Dipole moment values used for calculating the contributions from the hydrophobic force (Eq. [13]).

θ_a	$\mu \times 10^3$ (Debye)	C_o (mN/m)	D_o (nm)
75^o	1.0	-	-
83^o	1.5	-	-
92^o	8.0	-	-
100^o	10	-160	5
105^o	25	-175	8.0
109^o	35	-210	13.5

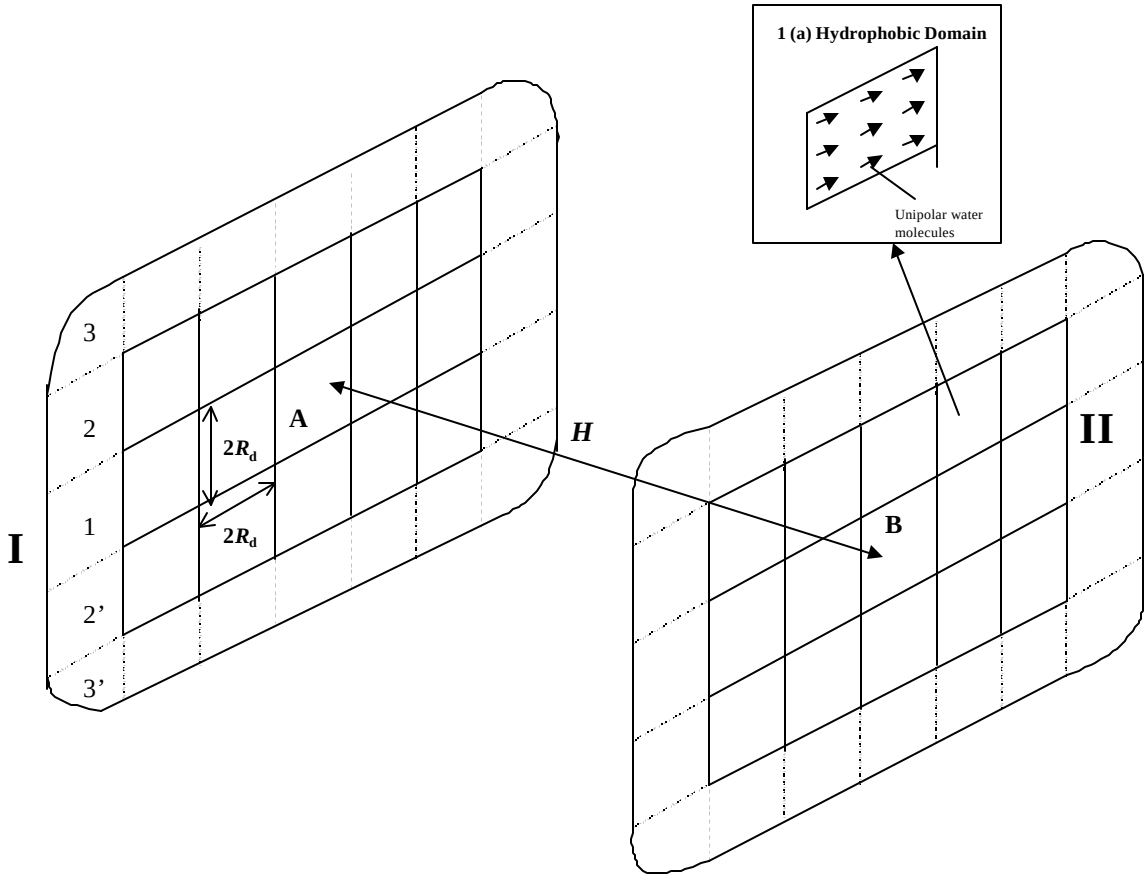

Figure 6.1. A schematic representation of two infinitely parallel plates interacting in a polar solvent such as water. The squares on the surfaces represent hydrophobic domains. The inset, 1(a) shows the unidirectional orientation of water molecules on a hydrophobic domain.

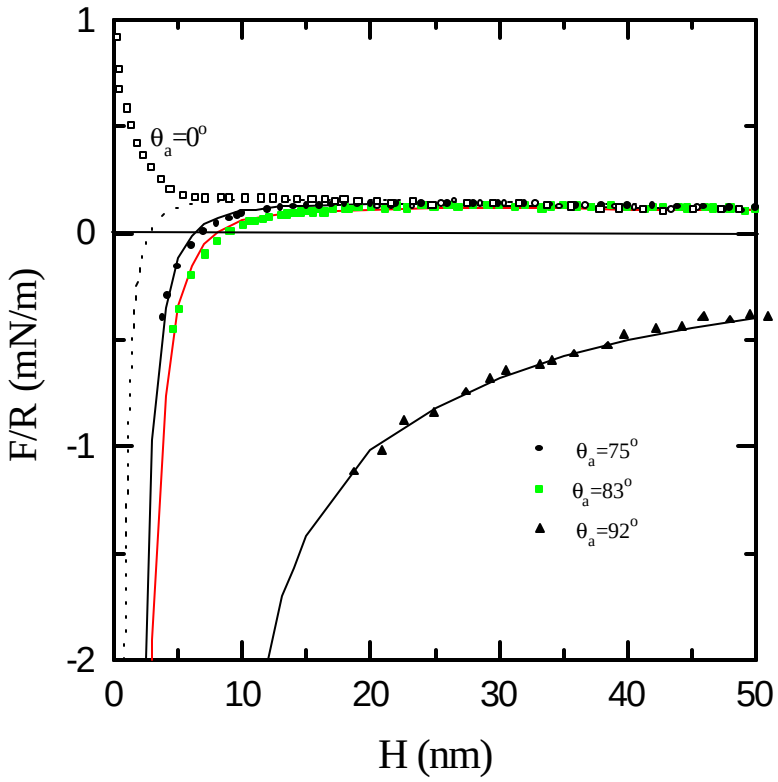

Figure 6.2. Results of the AFM force measurements conducted with silanated glass spheres and silica plates. The force, *F*, is normalized by the radius of the sphere, *R*, and plotted versus the separation distance, *H*. Each force curve was obtained using a sphere and silica plate silanated with octadecyltrichlorosilane (OTS) under identical conditions so that both exhibited the same contact angle: (□) 0^o, (•) 75^o, (■) 83^o, and (▲) 92^o. The dashed line represents a DLVO fit of the data (for $\theta_a=0^o$) with $A_{131}=8\times10^{-21}$ J, $\psi_1=-60$ mV and $\kappa^{-1}=94$ nm. The solid line represents an extended DLVO fit of the data [Eq.14]. Contributions from the hydrophobic force were calculated using Eq. [13]. The dipole moment values are given in Table 6.1.

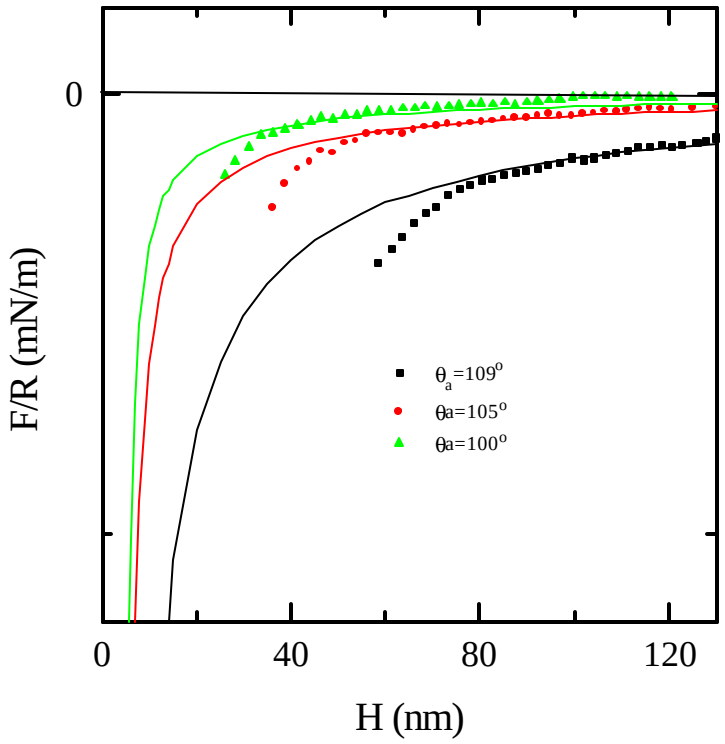

Figure 6.3. The *F/R vs H* curves obtained for the interaction of silanated glass spheres and silica plates. Each force curve was obtained using a sphere and silica plate silanated with octadecyltrichlorosilane (OTS) under identical conditions so that both exhibited the same contact angle: (■) 109°, (●) 105° and (▲) 100°. The solid line represents an extended DLVO fit of the data [Eq.14]. The values of F_e and F_d are the same as those used in Figure 6.2. Contributions from the hydrophobic force were calculated using Eq. [13]. The dipole moment values are given in Table 6.1

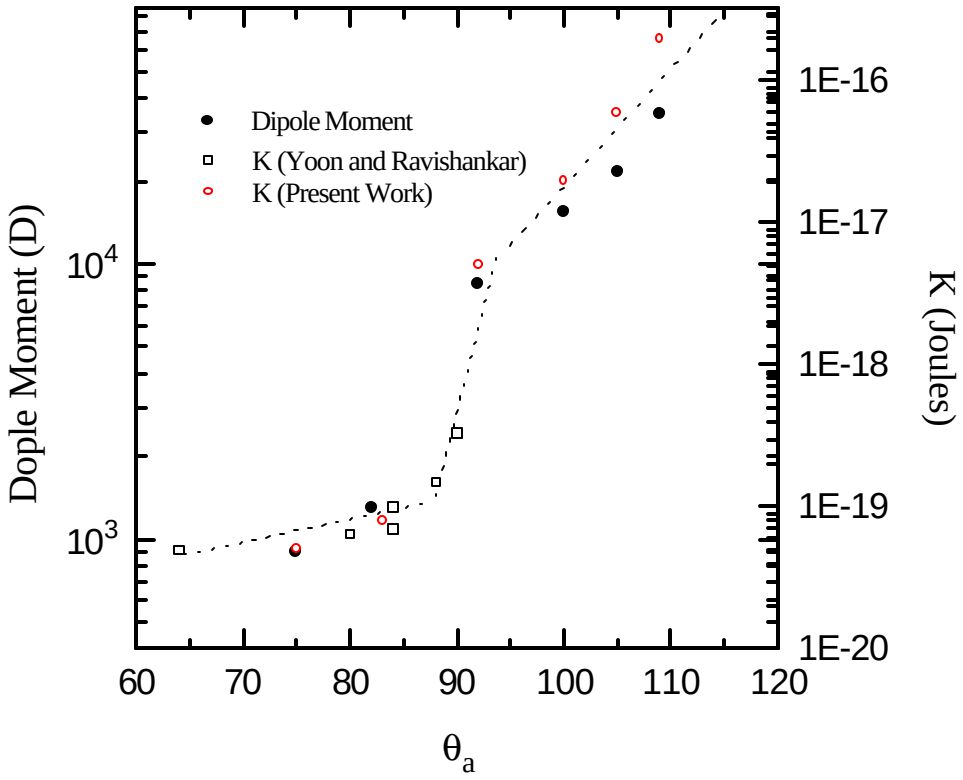

Figure 6.4. Dipole moment values obtained from Figures 2 and 3 plotted as a function of contact angle θ_a.

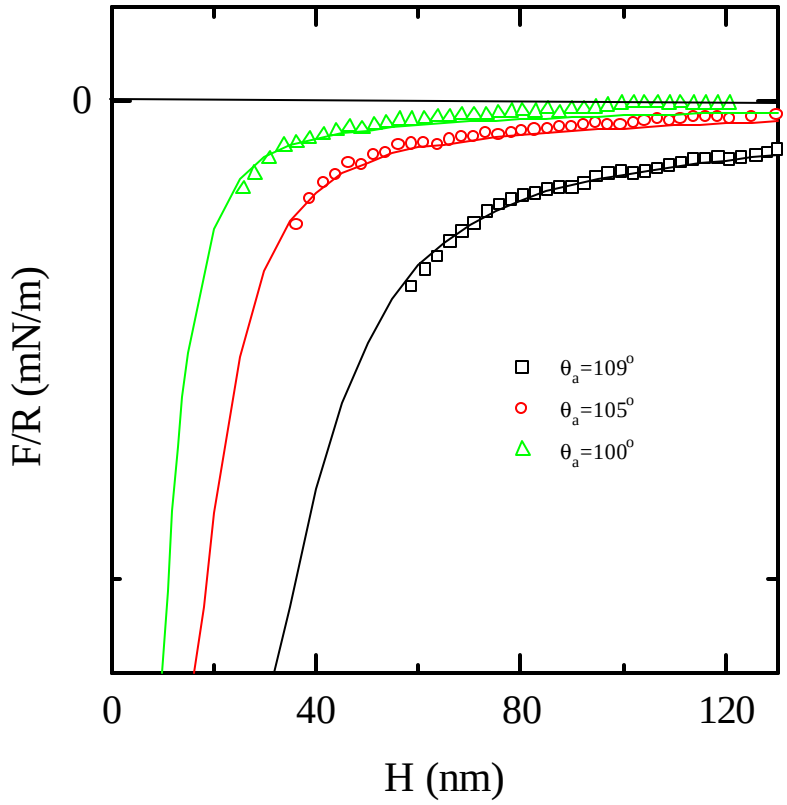

Figure 6.5. The *F/R vs H* curves obtained for the interaction of silanated glass spheres and silica plates. The silanated surfaces exhibit θa=100, 105 and 109o. The solid line represents an extended DLVO fit of the data. Contributions from the hydrophobic force were calculated using Eq. [15] which incorporates contributions from both cavitation and dipole correlation mechanisms.